

2- μm Narrow Linewidth All-Fiber DFB Fiber Bragg Grating Lasers for Ho- and Tm-Doped Fiber-Amplifier Applications

Wiktor Walasik¹, Daniya Traoré², Alexandre Amavigan³, Robert E. Tench⁴, *Senior Member, IEEE*, Jean-Marc Delavaux, and Emmanuel Pinsard

Abstract—We report the design and performance of a single frequency all-fiber distributed feedback (DFB) laser sources employing fiber Bragg gratings (FBGs) emitting in the 2- μm region. Output powers up to 65 mW CW and optical signal-to-noise ratios of >65 dB/0.05 nm are obtained. The emission wavelength of the DFB-FBG laser can be fine-tuned with picometer accuracy over a range of 0.6 nm by controlling the pump power and laser temperature. The single frequency source is amplified with polarization-maintaining Ho- or Tm-doped fiber amplifiers to an output power of 1 W CW at 2051 nm or 0.7 W CW at 2039 nm. Heterodyne measurements yield instantaneous laser linewidths of 5 kHz FWHM for both native and amplified signals.

Index Terms—Fiber amplifier, fiber laser, narrow linewidth, distributed feedback fiber Bragg grating, heterodyne measurement, LIDAR.

I. INTRODUCTION

THE development of simple, compact, and robust single frequency laser sources near 2.05 μm is important for many emerging applications including LIDAR [1]–[3], spectral sensing [4]–[6], coherent lightwave systems, and WDM transmission [7]. Most previous works on single frequency sources in the 2000 nm band have concentrated on packaged semiconductor lasers [8]–[11] and fiber based devices employing distributed Bragg reflector (DBR) technology [12]–[17]. However, semiconductor lasers offer output powers of only a few mW, and are characterized by emission linewidths of the order of a few MHz which renders them not suitable for coherent lightwave systems. For DBR lasers, splice losses and temperature induced mode-hops limit stability and prevent optimum single-frequency operation. With simple fabrication, low loss, and robust design,

distributed feedback fiber Bragg grating (DFB-FBG) lasers offer good stability and enable reliable single frequency operation with a narrow linewidth, therefore presenting a highly attractive and low cost alternative to semiconductor and DBR sources and semiconductor lasers in applications for amplifiers and coherent systems [18], [19]. Moreover, in contrast to semiconductor DFB lasers that are commercially available only at selected wavelengths in the 2 μm regime, the DFB-FBG lasers can be rapidly designed and fabricated at a wavelength of choice in the thulium and holmium emission bands [20]. While some work on 2 μm band DFB-FBG lasers has been previously reported for wavelengths as low as 1.91 μm up to 2.8 μm [20]–[23], a more comprehensive evaluation of these sources, particularly in a polarization-maintaining (PM) fiber in the vicinity of 2.05 μm , is desirable as they will make them practical seeders for PM fiber amplifier configurations.

In this paper, we describe the design and detailed performance of compact and stable single frequency DFB-FBG lasers emitting at 2051 and 2039 nm. Up to 65 mW of output power was recorded in a single mode operation. The lasers show high OSNR of above 62 dB/0.1 nm and their wavelength can be tuned with a picometer precision using thermal of pump-power tuning. The instantaneous linewidth of 5 kHz was measured using a heterodyne technique, corresponding to the coherence length of 20 km. The signal from DFB-FBG laser source was amplified to 1 W CW output power at 2051 nm with a Ho-doped fiber amplifier (HDFEA) master oscillator power amplifier (MOPA) configuration. Amplification with a Tm-doped fiber amplifier (TDFEA) resulted in up to 0.7 W of CW output power at 2039 nm and enabled measurement of the amplified linewidth. No linewidth degradation upon amplification was observed.

II. EXPERIMENTAL SETUP

Fig. 1 presents the schematic of a typical standard fiber DFB-FBG laser and the experimental setup used for its characterization. The DFB-FBG (ixblue IXC-CLFO-2000) consists of a few-centimeter-long piece of active Tm-doped fiber in which a DFB-FBG grating is written. For the DFB-FBG under investigation emitting at 2051 nm, the active fiber was 80 mm long and the length of the grating was 60 mm. Apodization techniques for the gratings yield an effective cavity length of 25 mm and a longitudinal mode spacing of 4.0 GHz. The reflectivities of the high- and low-reflection sides are $R_{\text{HR}} = 99.97\%$, $R_{\text{LR}} = 99.0\%$, respectively, at the wavelength of 2051 nm. The

Manuscript received January 5, 2021; revised March 10, 2021 and April 26, 2021; accepted May 5, 2021. Date of publication May 11, 2021; date of current version August 2, 2021. (Corresponding author: Wiktor Walasik.)

Wiktor Walasik, Alexandre Amavigan, Robert E. Tench, and Jean-Marc Delavaux are with the CYBEL LLC, Bethlehem, PA 18018 USA (e-mail: wiktor.walasik@cybel-llc.com; alexandre.amavigan@cybel-llc.com; robert.tench@cybel-llc.com; jm@cybel-llc.com).

Daniya Traoré was with Cybel LLC, Bethlehem, PA 18018 USA and now she is with the École Nationale Supérieure des Sciences Appliquées et de Technologie, 22305 Lannion, France (e-mail: daniya-traore@outlook.fr).

Emmanuel Pinsard is with ixblue Photonics, 22300 Lannion, France (e-mail: emmanuel.pinsard@ixblue.com).

Color versions of one or more figures in this article are available at <https://doi.org/10.1109/JLT.2021.3079235>.

Digital Object Identifier 10.1109/JLT.2021.3079235

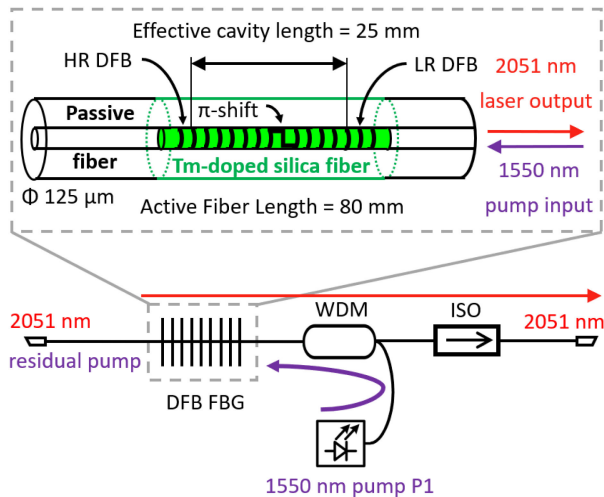


Fig. 1. Schematic of the DFB–FBG laser (top) and the topology of the system used for its characterization (bottom).

spectral full-width half-maximum (FWHM) of the high- and low-reflection gratings are 0.25 nm or 18 GHz and 0.34 nm or 24 GHz, respectively. A π phase-shift of the index modulation periodicity is written into the cavity, leading to robust single frequency operation of the laser. Passive fiber pigtailed (iXblue IXF-PAS-6-130-0.21) couple light into and out of the laser cavity.

The setup schematically shown in the bottom of Fig. 1 enables us to characterize the DFB–FBG laser performance. The DFB–FBG is pumped either by a 250 mW semiconductor (SC) laser pump (P1) at $\lambda = 1550$ nm or by a 1 W fiber laser (FL) at $\lambda = 1567$ nm via a wavelength division multiplexer (WDM) in a counter-pumped configuration. The isolator (ISO) at the output of the laser suppresses unwanted reflections into the laser cavity. The residual pump and the co-pumped emission can be accessed at the other side of the grating.

III. EXPERIMENTAL RESULTS

A. Performance of a Non-PM DFB–FBG at 2051 nm

We first investigate the performance of a non-polarization maintaining (non-PM) DFB–FBG laser emitting at $\lambda = 2051$ nm and pumped by a 1550 nm SC pump diode P1 (Lumentum S34). The output power from the DFB–FBG laser (P_s) as a function of the pump power (P_{P1}) is shown by the red curve in Fig. 2(a). The laser delivers 14.5 mW of power P_s at the maximum pump power $P_{P1} = 240$ mW, yielding an optical-to-optical efficiency $\eta = \Delta P_s / \Delta P_{P1}$ of 6.3%. The lasing threshold was measured to be $P_{P1} = 4$ mW. Next, the same DFB–FBG laser was pumped by a FL emitting at 1567 nm. At $P_{P1} = 800$ mW, the signal power reached $P_s = 65$ mW resulting in the efficiency $\eta = 8.5\%$. For FL pumping at 1567 nm efficiencies of up to 10.4% were observed. The increased pumping efficiency is a result of the pump wavelength of the fiber laser selected to be closer to the optimum absorption of the Tm-doped fiber. The single mode signal powers measured here from the DFB–FBG laser are more than an order of magnitude larger than these typically obtained for semiconductor seed laser diodes.

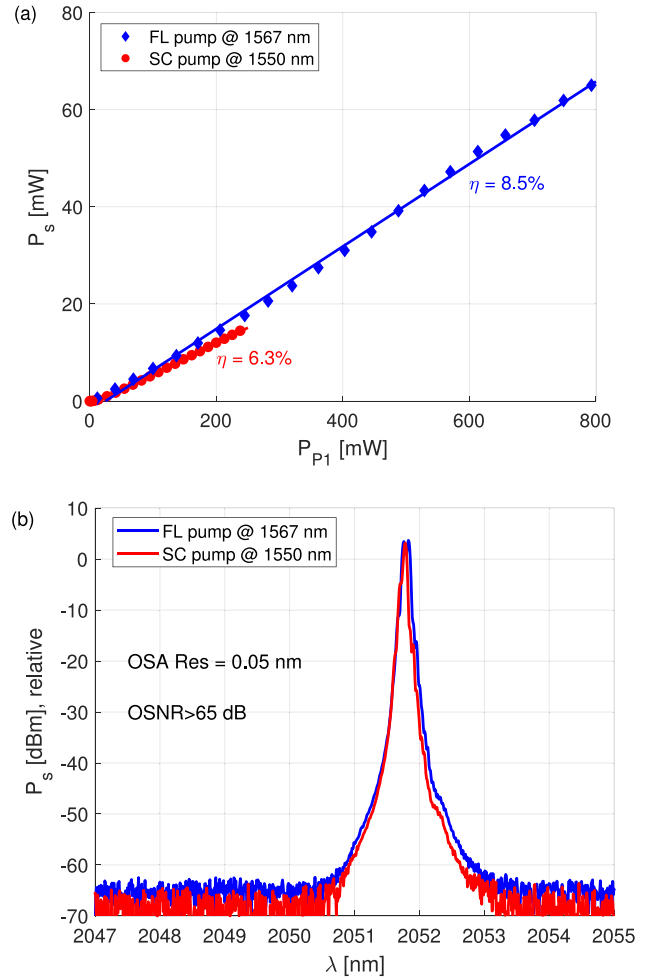


Fig. 2. (a) Output power P_s of a DFB–FBG laser as a function of the pump power P_{P1} for two different pump lasers. (b) Output spectra of the 2051 nm DFB–FBG laser for different types of pump.

Fig. 2(b) shows the spectra of the 2051-nm laser cavity measured for two different types of pump laser P1: the 1550 nm SC Lumentum laser and a 1567 nm FL. For both pumps, the signal is centered at 2051.8 nm and has an optical signal-to-noise ratio (OSNR) larger than 62 dB/0.1 nm. The OSNR is measured as a ratio between the power of the signal and the (interpolated) power of the amplified spontaneous emission (ASE) at the signal wavelength. We note that the spectral performance of the DFB–FBG laser is found to be quite similar for these two different types of pump sources indicating that fiber-laser pumps can successfully be used to power the single-frequency laser. The spectra shown in Fig. 2(b) are limited by the OSA resolution and do not allow for a precise estimation of the DFB–FBG laser linewidth. As described in Section III-D below, the instantaneous laser linewidth measured using a heterodyne technique was found to be 5 kHz. In the future, we plan to measure the $1/f$ noise distribution with an electrical spectrum analyzer (ESA) and contrast the results obtained for both types of pump lasers used in this work.

Fig. 3 shows the dependence of the central signal wavelength λ_s on the pump power P_{P1} of the FL. Initially, the bare fiber containing the DFB–FBG was in contact with an aluminum plate

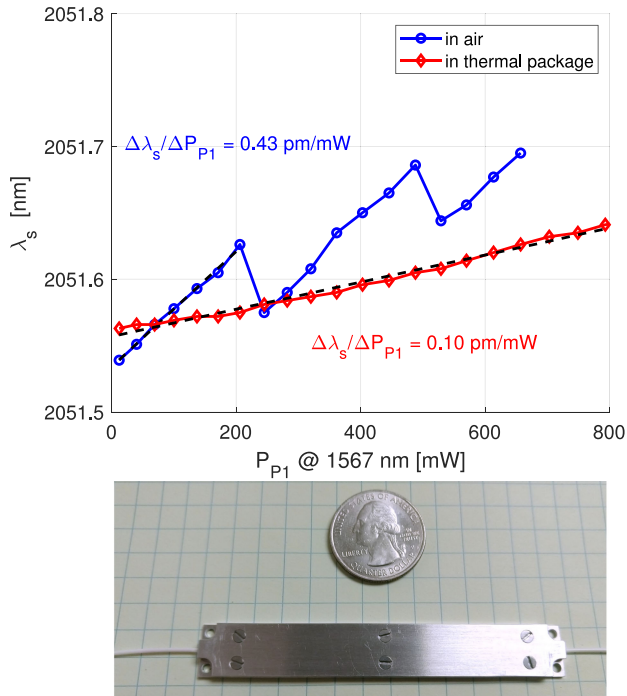


Fig. 3. Peak signal wavelength λ_s for a DFB–FBG laser pumped by a FL as a function of the pump power P_{P1} for the DFB–FBG in ambient air (blue) and in thermal package (red). The picture below the plot shows the photo of a thermal package with a US quarter dollar coin for scale.

but was surrounded by ambient air at the room temperature of 25°C. The dependence of λ_s on P_{P1} in this case is shown by the blue curve in Fig. 3. We observe that for low pump powers $P_{P1} < 200$ mW, the wavelength increases linearly with the slope $\Delta\lambda_s/\Delta P_{P1} = 0.43$ pm/mW. At $P_{P1} \approx 220$ mW, we observe a jump in the peak wavelength, which is a signature of the mode hopping of the DFB–FBG laser. Two closely spaced polarization modes are competing in the DFB–FBG laser. With the increase of the pump power (or temperature) the ratio of their amplitudes changes and as it crosses unity, a jump in the peak wavelength is observed.

Placing the DFB–FBG laser in a thermal package (shown at the bottom of Fig. 3) eliminates the mode hopping in the range of the pump powers studied here. The evolution of the peak signal wavelength for the DFB–FBG laser placed in the thermal package is shown by the red curve in Fig. 3. In addition to the absence of mode-hops, we also observe a reduced wavelength tuning slope. With the thermal package, the slope is reduced to the value of $\Delta\lambda_s/\Delta P_{P1} = 0.1$ pm/mW corresponding to approximately 7 MHz/mW, more than four-fold decrease compared to the DFB–FBG in ambient air. The DFB–FBG laser is much more stable with respect to operating parameters than 2000-nm band semiconductor lasers which typically exhibit 10 pm/mA current tuning.

It is clear from the data presented above that controlling the pump current (and therefore the pump power) enables a fine control of the wavelength. In that respect, the rapid change in pump power could help control the laser wavelength in a locking mechanism designed to stabilize the laser wavelength with sub-picometer accuracy.

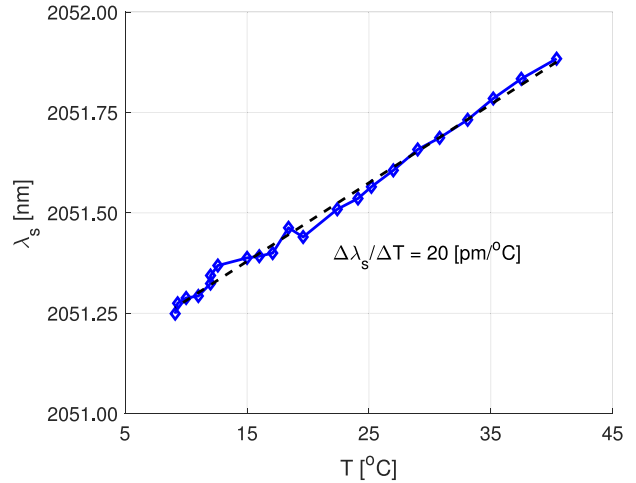


Fig. 4. Peak signal wavelength λ_s for a DFB–FBG laser pumped by a FL ($P_{P1} = 250$ mW) as a function of thermal package temperature T .

Placing the DFB–FBG laser in the thermal package enabled us to measure the influence of the laser temperature on the peak emission wavelength. We have used a Peltier thermoelectric cooler module placed under the thermal package to control the laser temperature. Figure 4 shows the dependence of the peak wavelength of the DFB–DBF laser on the temperature of the thermal package. By changing the temperature between 10 and 40°C we were able to change the peak wavelength by approximately 0.6 nm. The corresponding slope is $\Delta\lambda_s/\Delta T = 20$ pm/°C is approximately five times smaller than that the tunability of 100 pm/°C exhibited by a typical semiconductor laser operating in the 2 μ m band.

B. 2051 nm Signal Amplified by PM HDFA

Next, we evaluate the performance of the non-PM DFB–FBG laser emitting at 2051 nm as a seed for the two-stage PM HDFA. The schematic of the HDFA is shown in Fig. 5(a) and the details of the setup are described in Ref. [11], where the HDFA was used as a preamplifier stage. As the DFB–FBG laser is built using standard (non-PM) fiber, before coupling into a PM HDFA the polarization of the output signal is matched to the slow axis of the PM fiber using a polarization controller (PC), as shown in the inset of Fig. 5(b). The evolution of the HDFA output power (P_{out}) at 2051 nm as a function of the 1941-nm pump power of the HDFA (P_p) for three different levels of the input signal P_s is shown in Fig. 5(b). A maximum output power $P_{out} = 1$ W is obtained for $P_p = 5.2$ W. For the range of input power P_s studied here, the amplifier operated in saturation as evidenced by the fact that the level of output power was insensitive to P_s levels.

Figure 6(a) shows the spectra of the HDFA for the output power $P_{out} = 1$ W, measured for three different levels of the input signal power P_s . The width of the signal peak is limited by the resolution of the OSA and no apparent line broadening was observed. We also have not seen any signs of nonlinear processes such as stimulated Brillouin scattering (SBS). The level of the ASE decreases with the increase of the input signal power P_s leading to the OSNR as high as 64 dB/0.1 nm for $P_s = 11.4$ dBm. The residual 1941 nm pump is visible at the

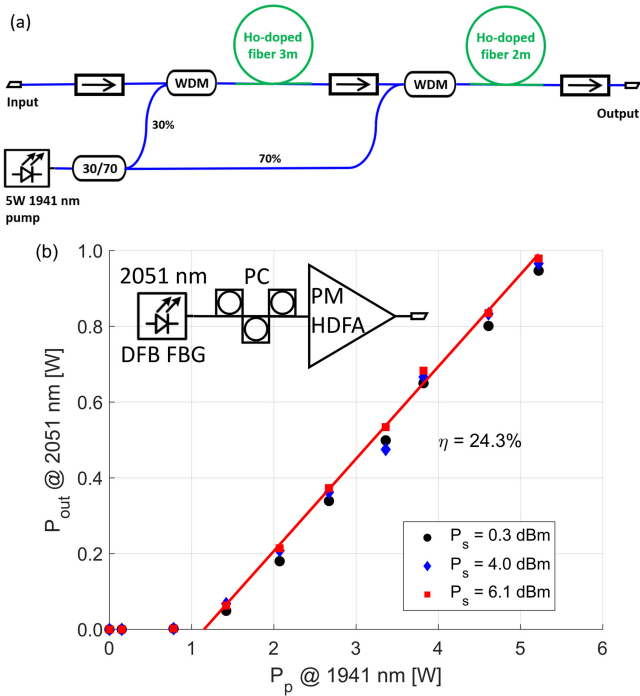


Fig. 5. (a) Topology of the two-stage PM HDFA. (b) Output power P_{out} of the HDFA as a function of pump power P_p for different levels of the input signal P_s .

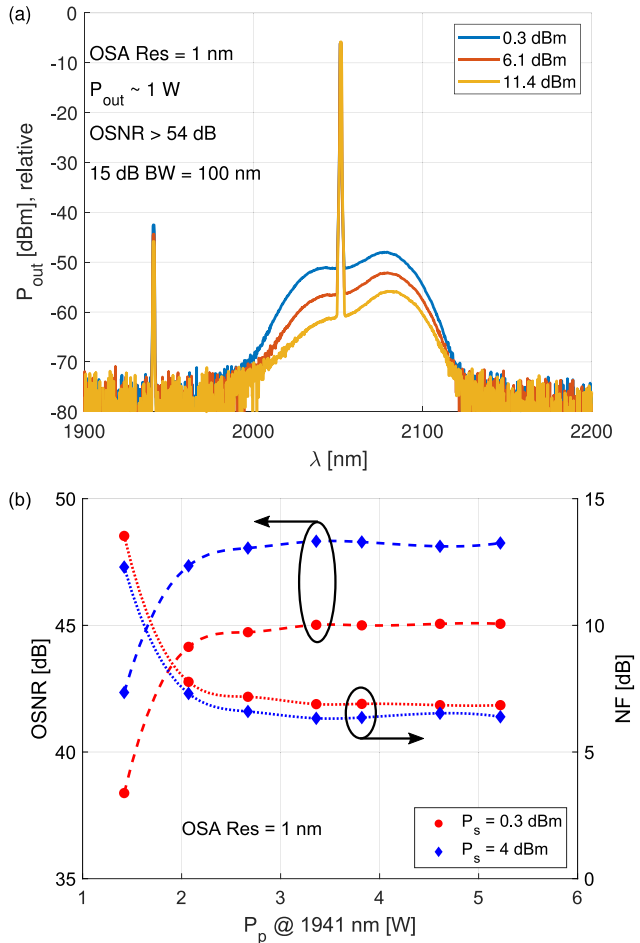


Fig. 6. (a) Spectra of the PM HDFA output for various input signal levels P_s . (b) OSNR and NF of the HDFA as a function of the pump power P_p .

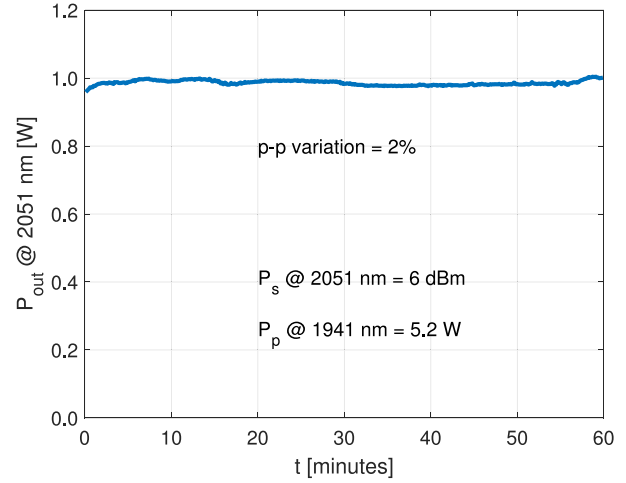


Fig. 7. Long-term stability of the output power P_{out} of the HDFA at 2051 nm.

level of -35 dBs with respect to the signal. At low P_s , the 15-dB bandwidth of the amplifier is 100 nm.

Figure 6(b) shows the OSNR and noise figure (NF) of the amplifier as a function of 1941 nm pump power P_p for two different levels of P_s . The noise figures were measured with the optical method using the optical spectrum analyzer. The OSNR increases with the increase of the pump power and it stabilizes for the pump power level $P_p > 2$ W. The OSNR of 55 (58) dB/0.1 nm is measured for the input signal level $P_s = 0.3$ (4.0) dBm. The NF decreases with the increase of the pump power and for $P_p > 2$ W it reaches the levels below 8 dB for both values of P_s used in the experiment.

Figure 7 shows the time evolution of the amplifier output power P_{out} measured for $P_s = 6$ dBm and $P_p = 5.2$ W. The maximum relative peak-to-peak variation of P_{out} is below 2% showing a good stability of both the signal power and the amplifier. Even though the DFB-FBG laser is made in a standard fiber, the stable operation of the amplifier provides an indirect measurement of the polarization stability of the non-PM DFB-FBG laser and suggests that the signal polarization constant in time. In the future, we plan to characterize directly the polarization stability of the signals emitted by the non-PM DFB-FBG lasers.

C. PM 2039 nm DFB-FBG Amplified by PM TDFA

In this section, we describe the use of a PM DFB-FBG laser as a seed for a PM TDFA. Here, we have used a DFB-FBG that was pigtailed with a PM fiber (iXblue IXF-PAS-PM-6-130-0.21) and was optimized to emit at 2039 nm. The DFB-FBG was integrated in a counter-pumped system that is illustrated at the bottom of Fig. 1. The laser was pumped with a SC laser diode emitting at 1550 nm with the pump power limited to 100 mW. In order to ensure a single mode laser operation, the PM 2039 nm DFB-FBG had been fabricated with a Tm-doped fiber with a lower doping concentration than the one used for the 2051 nm DFB-FBG. Moreover the coupling losses between the Tm-doped fiber and the PM pigtailed were higher than for the case of the non-PM fiber pigtailed. As a result the maximum power obtained from the 2039 nm DFB-FBG was limited to 1.5 mW, corresponding to the optical-to-optical efficiency $\eta \approx 1.5\%$.

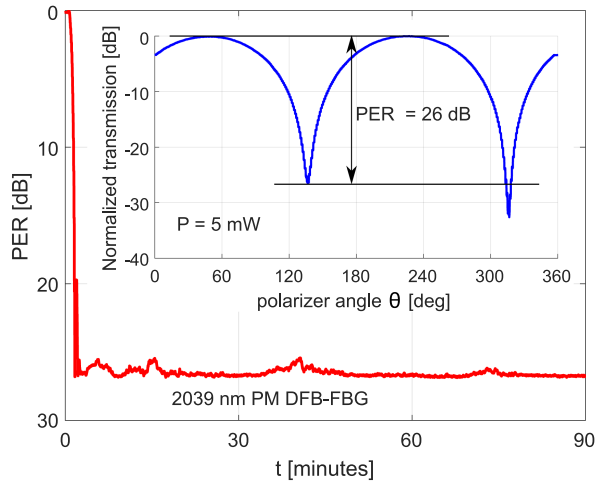


Fig. 8. Temporal dependence of the PER of the 2039 nm PM DFB FBG laser over a 90-minute period. The inset shows the dependence of the power transmitted through the polarizer versus the polarizer angle θ .

We have characterized the polarization extinction ratio (PER) of the PM 2039 nm DFB–FBG laser at the output of a fast-axis blocking isolator made with a PM Panda fiber. The laser output was collimated and transmitted through a 2- μm -band rotating linear thin film polarizer (Thorlabs LPNIRA with polarization rejection ratio of 40 dB) and detected by a high sensitivity photodetector (Thorlabs S148 C).

The inset of Fig. 8 shows the typical dependence of the measured normalized extinction ratio versus the rotation angle of the polarizer $0 \leq \theta \leq 360^\circ$ for an input power of 5 mW. The measured PER value, computed as a ratio of maximum to minimum power detected, was larger than 26 dB. Similar PER values were measured for laser output setting from 100 μW to 20 mW, that were achieved by adjusting the 1550 nm pump power to the DFB–FBG laser.

In addition, the temporal stability of the PER value was measured through the polarizer for maximum and minimum light transmission. For maximum light transmission, the measured power changed by less than 4% over 180 minutes, which indicated no significant variation in the polarization. In the second experiment, we first found the maximum transmission and then rotated the polarizer by 90° to reach a minimum. Then the power variation was monitored over the period of 90 minutes, as shown in Fig. 8. The minimum transmitted power remained relatively stable, corresponding to PER values ranging from 25 to 27 dB. This process was repeated at the location of both minima found in our visibility curve and led to the same outcome.

Next, we attempted a direct PER measurement of the PM FBG–FBG laser fiber output by removing the PM isolator and obtained a PER value of 14 ± 4 dB. This measurement was difficult to implement due to power output instability caused by the system back-reflections to the laser. Overall, our isolated 2 μm PM DFB–FBG laser exhibits a stable output power with a PER value larger than 25 dB which makes it a good candidate as a seeder for thulium- or holmium-doped fiber amplifiers.

The signal from the isolated output of the PM DFB–FBG laser was used as a seed for the PM TDFA shown in the inset of Fig. 9(a). The amplifier consisted of a 5-m-long PM double clad (DC) Tm-doped fiber (iXblue IXF-2CF-Tm-PM-6-130-0.21)

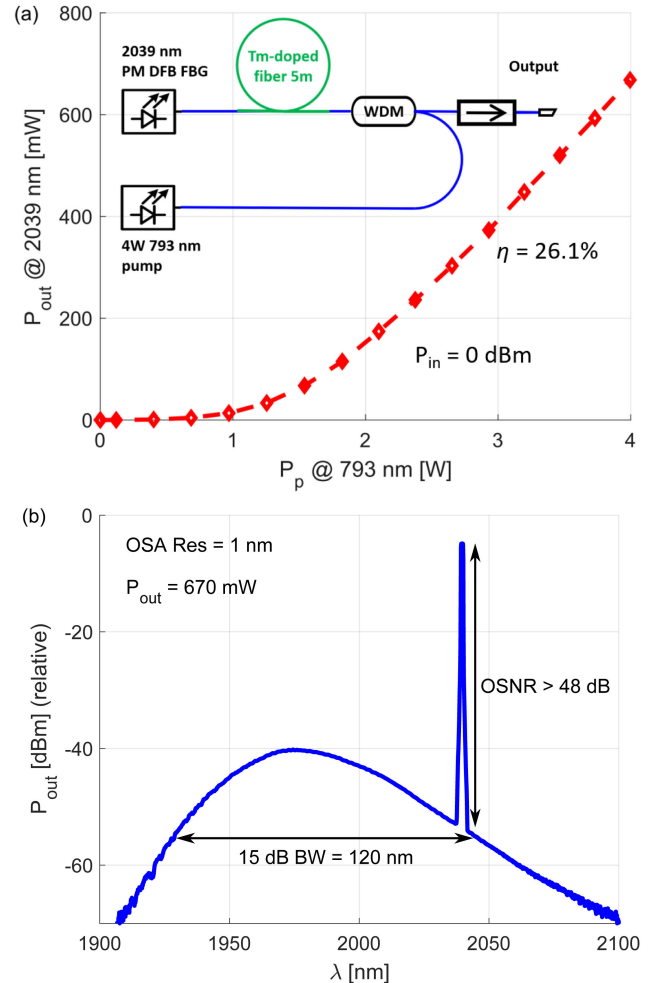


Fig. 9. (a) Output power P_{out} of the PM TDFA as a function of pump power P_p for signal at 2039 nm with the input power of $P_s = 0$ dBm. (b) Spectrum of the TDFA output for $P_s = 0$ dBm.

pumped by a 4 W 793 nm multimode pump diode via WDM in a counter-pumped configuration. The output of the amplifier was isolated to prevent the parasitic reflections.

The output power at 2039 nm as a function of the 793 nm pump power P_p is shown in Fig. 9(a) for the input signal $P_{\text{in}} = 0$ dBm. The power of up to 670 mW was measured at the pump level of 4 W, resulting in the slope efficiency of $\eta \approx 26\%$.

The spectrum of the TDFA operating at 2039 nm with the input signal power $P_s = 0$ dBm is shown in Fig. 9(b). We have measured the OSNR of 58 dB/0.1 nm and the 15-dB bandwidth of the amplifier is 120 nm.

Two PM 2039 nm DFB–FBG lasers and two TDFA with the architectures shown in the inset of Fig. 9(a) were used for the measurements of the native and amplified linewidths, as described in the next section.

D. Linewidth Measurements

In order to measure the linewidth of the DFB–FBG lasers we have constructed a polarization maintaining (PM) heterodyne system schematically shown in Fig. 10(a). The signals from two lasers emitting at closely spaced wavelengths (within the bandwidth of the photodiode (PD) and the electrical spectrum

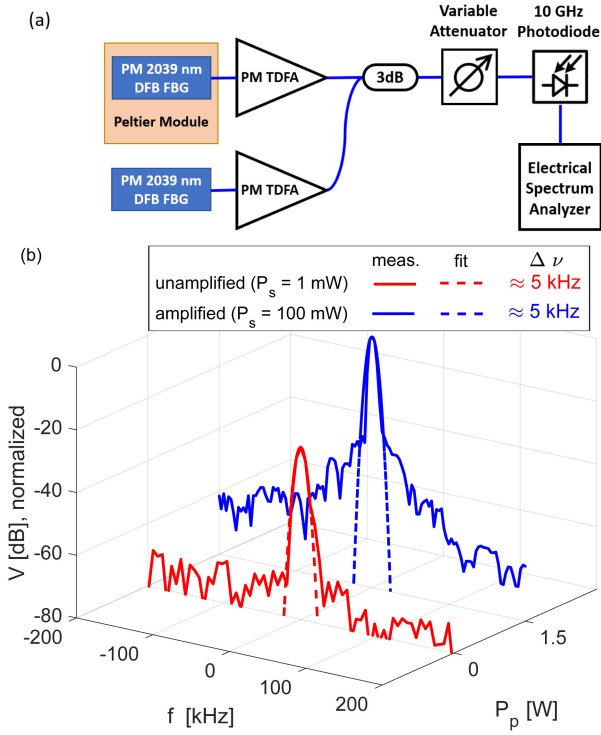


Fig. 10. (a) Schematic of the polarization maintaining heterodyne setup used for the linewidth measurements. (b) Spectrum of the recorded beat-notes of the signals before (red) and after amplification (blue). Beat-note spectra were shifted to zero-frequency.

analyzer (ESA)) are mixed using a PM 3-dB coupler. The mixed signal is attenuated by a variable attenuator in order to avoid saturation of the PD. The optical heterodyne signal is transformed into electrical signal by a fast extended InGaAs PD (Electro-Optics Technology ET-5000F). The spectrum of the electrical signal was observed and recorded by the ESA (Keysight N9010B EXA).

We have used the signals from two PM DFB–FBG lasers emitting at in the vicinity of 2039 nm. In order to bring the wavelengths of the two lasers within the bandwidth of the PD, the temperature of one of the lasers was controlled by a Peltier thermoelectric cooler module, allowing to tune the emission wavelength. The signal from the two DFB–FBG lasers was transmitted through two TDFAs, with the architecture shown in the inset of Fig. 9(a).

In the first experiment, the instantaneous linewidth of the unamplified DFB–FBG laser was measured. To this end, the signal from the two lasers, each emitting the power $P_s = 1$ mW, was transmitted through unpowered TDFAs ($P_p = 0$ W). In this case, the Tm-doped fiber acted as an attenuator for the 2039 nm signal. The recorded heterodyne signal is shown by a red curve in Fig. 10(b). The instantaneous laser linewidth of 5 kHz FWHM was measured based on the Gaussian fit to the heterodyne data. This is consistent with previous linewidth measurements of 2000-nm band DFB–FBG lasers of ≈ 10 –30 kHz [20], [22], [23].

Finally, the linewidth of the amplified signal was measured. Both PM TDFAs were pumped with the pump powers of $P_p = 1.5$ W, resulting the signal power from each DFB–FBG laser

being amplified to the level of $P_s = 100$ mW. The heterodyne signal obtained for the amplified lasers is shown by a blue curve in Fig. 10(b). The measured instantaneous linewidth of the amplified signal is 5 kHz FWHM showing that the linewidth is not broadened by the amplification process. For the amplified signal, the heterodyne spectrum shows two sidebands approximately 200 kHz away from the main peak with the amplitudes more than 50 dBs below the main peak. Long term heterodyne measurement of the linewidth would require the wavelength to be locked to an atomic absorption line. Alternatively, a self-heterodyne method employing an amplifier loop could be used [24], [25], however the high fiber loss at 2 μ m might still make it difficult [26].

IV. CONCLUSION

We have reported the design and evaluation of single frequency DFB–FBG fiber lasers using Tm-doped fibers operating at 2051 and 2039 nm. Output powers up to 65 mW were obtained by pumping the FBG–DFB with ≈ 1550 nm light from either semiconductor or fiber-laser pump sources. Virtually no difference in single-frequency laser performance was observed with the two widely different pump sources, indicating that fiber-laser pumps can successfully be used in this sensitive single-frequency application. OSNR values of more than 62 dB/0.1 nm and heterodyne linewidths of 5 kHz FWHM were measured for the single-frequency DFB–FBG lasers. The DFB–FBG lasers show a very good wavelength stability with respect to pump power and temperature. The variation of output wavelength was measured to be below 0.1 pm (7 MHz) per mW of pump power and less than 20 pm per $^{\circ}$ C. This allows for a more stable seed operation compared to the semiconductor counterparts and enable very fine wavelength tuning. For applications that require a stable wavelength operation independent of the environment temperature over a given temperature range, the DFB–FBG can be packaged in an athermal package, similarly to the athermal FBGs. Alternatively, for applications where precise wavelength control is not necessary, an uncooled package can be used while keeping the same optical performance and reducing the cost and complexity of the control layout.

Amplification of the single frequency DFB–FBG signal was demonstrated using a two-stage PM HDFA and a single stage PM T DFA. The output powers of 1 W at 2051 nm was achieved using the HDFA and up to 0.7 W at 2039 nm was measured with the T DFA. A long-term HDFA MOPA output power stability of 2% over 1 h was measured for the amplified 2051 nm source, indicating that the power and polarization state of this laser are stable with time. The amplified linewidth was calculated to be 5 kHz, assuming the Gaussian profile, and no linewidth degradation was observed. Moreover, no signs of nonlinear processes such as SBS were observed upon amplification.

Finally, we have demonstrated, in addition to previously reported standard (non-PM) DFB–FBG lasers, the use of fully PM DFB–FBG lasers. We have shown that these laser sources offered a PER better than 25 dB with very good polarization time-stability. Therefore, PM DFB-FBG lasers can be used as stable seed lasers in fully PM fiber amplifier configurations, which constitute a critical improvement when compared to the non-PM laser sources in their use in PM MOPA configurations.

The DFB–FBG lasers presented here can be designed to operate in a broad wavelength range covering the emission band of the Tm-doped fiber and spanning from 1900 nm to 2100 nm. In our other experiments (unpublished results), we have demonstrated the operation of the Tm-based DFB–FBGs at the wavelength of 1908 nm. One of the possible application of the DFB–FBG amplified lasers could be as a means of pumping in the 2 μm regime alternative to DBR fiber lasers. Moreover, future applications of this highly stable single-frequency laser source include LIDAR, spectral sensing, coherent lightwave systems, and WDM transmission in the 2 μm band.

REFERENCES

- [1] T. J. Wagener, N. Demma, J. D. Kmetec, and T. S. Kubo, “2 μm LIDAR for laser-based remote sensing: Flight demonstration and application survey,” *IEEE Aerosp. Electron. Syst. Mag.*, vol. 10, no. 2, pp. 23–28, Feb. 1995.
- [2] F. Gibert, P. H. Flamant, D. Bruneau, and C. Loth, “Two-micrometer heterodyne differential absorption lidar measurements of the atmospheric CO₂ mixing ratio in the boundary layer,” *Appl. Opt.*, vol. 45, no. 18, pp. 4448–4458, Jun. 2006.
- [3] S. Ishii *et al.*, “Coherent 2 μm differential absorption and wind lidar with conductively cooled laser and two-axis scanning device,” *Appl. Opt.*, vol. 49, no. 10, pp. 1809–1817, Apr. 2010.
- [4] G. D. Spiers *et al.*, “Atmospheric CO₂ measurements with a 2 μm airborne laser absorption spectrometer employing coherent detection,” *Appl. Opt.*, vol. 50, no. 14, pp. 2098–2111, May 2011.
- [5] J. A. Nwaboh, O. Werhahn, P. Ortwein, D. Schiel, and V. Ebert, “Laser-spectrometric gas analysis: CO₂-TDLAS at 2 μm ,” *Meas. Sci. Technol.*, vol. 24, no. 1, Dec. 2012, Art. no. 0 15202.
- [6] Y. Ueda *et al.*, “2- μm active DBR laser for wide-tuning-range CO₂ gas sensing,” in *Proc. IEEE Int. Semicond. Laser Conf.*, 2018, pp. 1–2.
- [7] H. Zhang *et al.*, “Dense WDM transmission at 2 μm enabled by an arrayed waveguide grating,” *Opt. Lett.*, vol. 40, no. 14, pp. 3308–3311, Jul. 2015.
- [8] J. Liu, H. Shi, K. Liu, Y. Hou, and P. Wang, “210 W single-frequency, single-polarization, thulium-doped all-fiber MOPA,” *Opt. Exp.*, vol. 22, no. 11, pp. 13 572–13 578, 2014.
- [9] L. Li, B. Zhang, K. Yin, and J. Hou, “75 W single-frequency, thulium-doped fiber laser at 2.05 μm ,” *Laser Phys. Lett.*, vol. 12, no. 9, 2015, Art. no. 0 95103.
- [10] R. E. Tench, A. Amavigan, J.-M. Delavaux, T. Robin, B. Cadier, and A. Laurent, “Novel miniature 2 μm Watt-level PM single clad Tm-doped fiber amplifier,” in *Proc. Fiber Lasers XVII: Technol. Syst.*, 2020, pp. 102–106.
- [11] R. E. Tench, C. Romano, J. Delavaux, R. Lenox, D. Byrne, and K. Carney, “In-depth studies of the spectral bandwidth of a 25 W 2 μm band PM hybrid Ho- and Tm-doped fiber amplifier,” *J. Lightw. Technol.*, vol. 38, no. 8, pp. 2456–2463, 2020.
- [12] Z. Zhang, A. J. Boyland, J. K. Sahu, W. A. Clarkson, and M. Ibsen, “High-power single-frequency thulium-doped fiber DBR laser at 1943 nm,” *IEEE Photon. Technol. Lett.*, vol. 23, no. 7, pp. 417–419, Apr. 2011.
- [13] S. Fu *et al.*, “2 μm single frequency fiber laser based on thulium-doped silica fiber,” in *Proc. Fiber Lasers XIII: Technol., Syst., Appl.*, 2016, pp. 218–223.
- [14] C. Yang *et al.*, “Short all Tm-doped germanate glass fiber MOPA single-frequency laser at 1.95 μm ,” *Opt. Exp.*, vol. 24, no. 10, pp. 10956–10961, May 2016.
- [15] S. Fu *et al.*, “Compact hundred-mW 2 μm single-frequency thulium-doped silica fiber laser,” *IEEE Photon. Technol. Lett.*, vol. 29, no. 11, pp. 853–856, Jun. 2017.
- [16] S. Fu *et al.*, “Review of recent progress on single-frequency fiber lasers [invited],” *J. Opt. Soc. Amer. B*, vol. 34, no. 3, pp. A49–A62, Mar. 2017.
- [17] T. Yin, Y. Song, X. Jiang, F. Chen, and S. He, “400 mW narrow linewidth single-frequency fiber ring cavity laser in 2 μm waveband,” *Opt. Exp.*, vol. 27, no. 11, pp. 15 794–15 799, May 2019.
- [18] M. Guionie *et al.*, “Delay-induced instability in phase-locked dual-polarization distributed-feedback fiber lasers,” *Phys. Rev. A*, vol. 101, Apr. 2020, Art. no. 0 43843.
- [19] M. Guionie *et al.*, “Beat note stabilization in dual-polarization DFB fiber lasers by an optical phase-locked loop,” *Opt. Exp.*, vol. 26, no. 3, pp. 3483–3488, Feb. 2018.
- [20] A. A. Wolf *et al.*, “All-fiber holmium distributed feedback laser at 2.07 μm ,” *Opt. Lett.*, vol. 44, no. 15, pp. 3781–3784, 2019.
- [21] D. Gapontsev *et al.*, “20 W single-frequency fiber laser operating at 1.93 μm ,” in *Proc. Conf. Lasers Electro-Opt./Quantum Electron. Laser Sci. Conf. Photon. Appl. Syst. Technol.*, 2007, Paper CF15.
- [22] M. Bernier, V. Michaud-Belleau, S. Levasseur, V. Fortin, J. Genest, and R. Vallée, “All-fiber DFB laser operating at 2.8 μm ,” *Opt. Lett.*, vol. 40, no. 1, pp. 81–84, 2015.
- [23] L. Antoni-Micollier *et al.*, “Watt-level narrow-linewidth fibered laser source at 852 nm for FIB application,” *Opt. Lett.*, vol. 43, no. 16, pp. 3937–3940, Aug. 2018.
- [24] J. W. Dawson, N. Park, and K. J. Vahala, “An improved delayed self-heterodyne interferometer for linewidth measurements,” *IEEE Photon. Technol. Lett.*, vol. 4, no. 9, pp. 1063–1066, Sep. 1992.
- [25] M. Chen, Z. Meng, J. Wang, and W. Chen, “Ultra-narrow linewidth measurement based on Voigt profile fitting,” *Opt. Exp.*, vol. 23, no. 5, pp. 6803–6808, Mar. 2015.
- [26] Y. Chen *et al.*, “Multi-kilometer long, longitudinally uniform hollow core photonic bandgap fibers for broadband low latency data transmission,” *J. Lightw. Technol.*, vol. 34, no. 1, pp. 104–113, 2016.

Wiktor Walasik was born in Jawor, Poland, in 1987. He received the M.S. degree in physics from Wrocław University and Technology, Wrocław, Poland and from École normale supérieure Cachan, Cachan, France, in 2011, and the Ph.D. degree in photonics from Aix-Marseille University, Marseille, France, in 2014.

From 2015 to 2018, he was a Research Assistant Professor with the University at Buffalo, SUNY, Buffalo, NY, USA, and from 2018 to 2019, he was a Postdoctoral Associate with Duke University, Durham, NC, USA. Since 2020, he has been a Technical Program Manager with CYBEL LLC, Bethlehem, PA, USA. He is the author of more than 30 articles and more than 20 conference presentations. His research interests include fiber lasers, nonlinear and super-symmetric optics, and metamaterials.

Dr. Walasik’s awards and honors include Aspen Institute Price in 2020, and the Best Oral Presentation at Phobia Annual Nanophotonics International Conference 2011.

Daniya Traorée, Author photograph and biography not available at the time of publication.

Alexandre Amavigan, Author photograph and biography not available at the time of publication.

Robert E. Tench (Senior Member, IEEE) was born in Pittsburgh, PA, USA, in 1957. He received the B.A. degree in physics from Swarthmore College, Swarthmore, PA, USA, in 1978, and the Ph.D. degree in physics from the Massachusetts Institute of Technology, Cambridge, MA, USA, in 1985.

He has conducted laser and fiber optics research and development with AT&T Bell Laboratories, Lucent Bell Laboratories, the National Security Agency, Johns Hopkins University, Baltimore, MD, USA, Cybel LLC, Bethlehem, PA, USA, and RET and Associates LLC. He is the author of more than 85 journal and conference papers, has nine current or pending patents, and has placed over a dozen products into manufacture.

Dr. Tench is a Senior Member of OSA and a Member of Sigma Xi.

Jean-Marc Delavaux, Author photograph and biography not available at the time of publication.

Emmanuel Pinsard, Author photograph and biography not available at the time of publication.